Dipole–dipole interactions among CH_3Cl molecules on Ru(001): Correlation between work function change and thermal desorption studies

T. Livneh,[a] Y. Lilach, and M. Asscher
Department of Physical Chemistry and the Farkas Center for Light Induced Processes, The Hebrew University, Jerusalem 91904, Israel

(Received 26 March 1999; accepted 21 September 1999)

Work function change measurements ($\Delta\Phi$) combined with temperature programmed desorption (TPD) were employed to study layer growth mechanism and the CH_3Cl dipole–dipole interactions on Ru(001), over the temperature range of 97 K–230 K. The activation energy for desorption (E_a) and the molecular dipole moment (μ) both decrease from 55.9 kJ/mol and 2.44 D, at the zero coverage limit, to 38.6 kJ/mol and 1.27 D, at one monolayer. This coverage dependence originates from strong dipolar lateral repulsion among neighbor CH_3Cl molecules. Using a model introduced by Maschhoff and Cowin (MC) [J. Chem. Phys. **101**, 8138 (1994)], the isolated adsorbed molecule's dipole moment, μ_0 (2.35 D) and polarizability $\alpha(8.1\times10^{-24}\,\mathrm{cm}^3)$, were extracted from TPD data. These values agree very well with μ_0 (2.12 D) and $\alpha(9.2\times10^{-24}\,\mathrm{cm}^3)$ obtained from work function change measurements by employing the same MC model. The ability to simulate both TPD and work function change data over a wide coverage range within the framework of a single electrostatic model has been demonstrated. It enabled better understanding of fine details of surface dipolar interactions. © *1999 American Institute of Physics.* [S0021-9606(99)70447-2]

I. INTRODUCTION

The adsorption and chemistry of methyl halides on single crystal surfaces have been the focus of many studies in recent years.[1,2] The importance of these molecules as a model for surface alkylation, and in particular their damaging role in atmospheric reactions, have motivated these studies. Under UHV conditions the reactivity toward C–X bond cleavage follows the trend I>Br>Cl on several catalytic metal surfaces. On Ru(001) CH_3I was found to completely dissociate upon adsorption at 100 K,[3] and CH_3Br to partly (55%) dissociate above 125 K.[4] In contrast, CH_3Cl does not dissociate on Ru(001), Pt(111),[5] or Pd(100)[6,7] surfaces.

Repulsive dipole–dipole interaction between parallel dipoles is the common reason for decreasing activation energy for desorption, E_a, as coverage increases. This was demonstrated in the case of alkali metals,[8] and molecules characterized by permanent dipole moments, like methyl halides.[9] The closely related induced dipole–dipole interactions in rare gases adsorption was studied as well.[10] Several electrostatic models were employed, which enabled the simulation of TPD spectra. The most recent and extensive model was developed by Maschhoff and Cowin (MC).[11] These authors have extended the Topping model[12] by taking into account the attractive interaction between the adsorbate and its surface image dipole, which is dominant at low coverages. At high coverages, repulsive interactions dominate, which lead to depolarization effects, resulting in the reduction of the adsorbate's dipole moment, μ.

The ability to follow work function change ($\Delta\Phi$) and TPD measurements under identical experimental conditions was shown to improve our understanding of the detailed fragmentation mechanism, prior to and during desorption of CH_3Br from Ru(001).[4] In that study dissociation pathways had been proposed and found to correlate well with HREELS measurements on CH_3I/Ru(001).[3] However, due to the extensive dissociation of CH_3Br and CH_3I on the Ru(001) surface, it was difficult to uniquely correlate work function change and TPD data, in the regime where the parent molecule's dissociation takes place. Such a procedure is possible in the case of CH_3Cl on Ru(001), due to the reversible molecular adsorption and the absence of dissociation at any coverage, and makes it an ideal system for the study of dipole–dipole interactions on single crystal surfaces.

A question arises whether dipole–dipole interactions among molecules adsorbed on conductive surfaces described by electrostatic expressions, e.g., the MC model, are accurate enough to predict the coverage dependent work function change and activation energy simultaneously with the same set of parameters. Previous efforts to predict the work function change upon monolayer completion [e.g., CH_3Cl on Cu(110)],[13] from TPD analysis based on a single work function change measurement,[14] were unsuccessful.[13]

The objectives of this work are twofold: (a) Correlate between the rate of desorption and the rate of work function change. Discrepancy between the two often originates from coverage dependence of the dipole moment. (b) Independently measure the coverage dependence of the activation energy for CH_3Cl desorption, $E_a(n)$, and that of the CH_3Cl dipole moment, $\mu(n)$, on the Ru(001) surface. Employing the MC model,[11] we then derive the coverage dependence of $\mu(n)$ from $E_a(n)$ data. The ability to correlate the two experimental observables using the MC electrostatic model can serve as a test case for the model completeness, and to

[a]Current address: Department of Physical Chemistry, Nuclear Research Center, Negev, P.O. Box 9001, Beer Sheva, Israel.

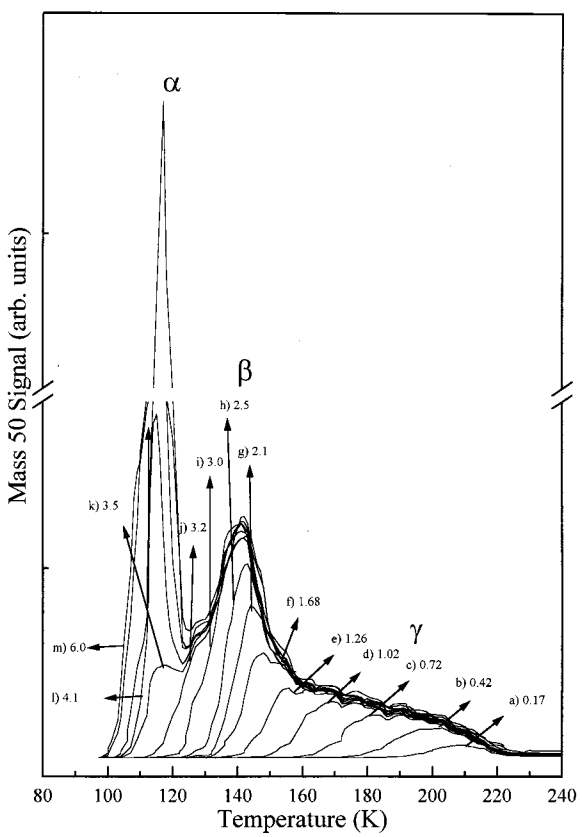

FIG. 1. Δp-TPD spectra of CH_3Cl from Ru(001) at the indicated exposures (L). The adsorption temperature was 97 K and the heating rate 2.1 K/s.

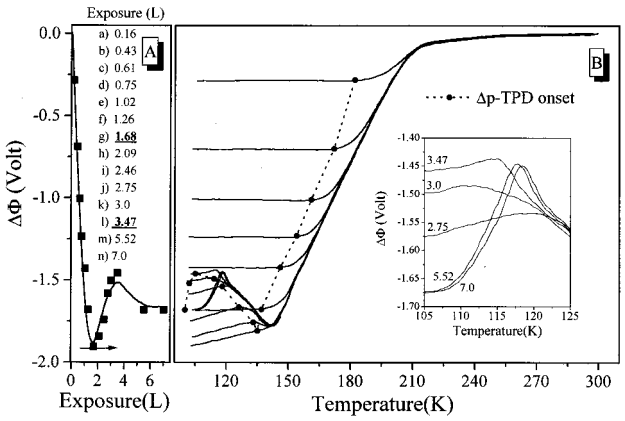

FIG. 2. (A) $\Delta\Phi_{ads}$ (work function change measurement during adsorption) of CH_3Cl on Ru(001) at 97 K (solid line). (B) $\Delta\Phi$-TPD of CH_3Cl from Ru(001) after the indicated exposures in Langmuirs. The adsorption temperature was 97 K and the heating rate 1.0 K/s. The initial value of $\Delta\Phi$ in the $\Delta\Phi$-TPD spectra and the onset temperatures for the corresponding Δp-TPD spectra are marked by filled squares (in A) and filled dots (in B), respectively. In the inset, the section in the $\Delta\Phi$-TPD spectra, which corresponds to the multilayer desorption temperature regime, is magnified.

weight the uncertainty, which originates from some of the simplifying assumptions included in the model.

II. EXPERIMENT

The experiments described here were performed in an ultra high vacuum (UHV) chamber with a base pressure of 1×10^{-10} Torr, obtained by a turbomolecular pump (520 l/s). Ar^+ ions at 600 V were used to sputter-clean the Ru(001) surface (typical sample current of 8 μA). A computer-controlled ac-resistive heating routine could control the sample heating rate or stabilize its temperature (±0.5 °K). At the same time signal is collected from either a quadrupole mass spectrometer (VG-MASSTORR DX) (QMS) to obtain normal TPD spectra (Δp-TPD), or from a Kelvin probe (Besocke Type-S) controller, to obtain $\Delta\Phi$-TPD spectra. The QMS was surrounded by Pyrex shroud with a 4 mm aperture to prevent contribution to the Δp-TPD from surfaces other then the sample.

The Ru(001) sample (a square piece, 8×8 mm, 1 mm thick) was cut from a single crystal rod to within 1° of the (001) crystallographic orientation, and was polished by standard metallurgical methods. Sample cleaning in UHV has been described elsewhere.[4] LEED from the clean and annealed surface showed very sharp hexagonal patterns. The sample was spot welded between two 0.5 mm diameter tantalum wires, and was attached to a liquid nitrogen reservoir, via copper feedthroughs, directly welded to the bottom of the Dewar. The temperature was monitored by a W5%Re–W26%Re thermocouple spot welded to the edge of the ruthenium sample.

CH_3Cl (99.5% pure) was further purified by a few freeze–pump–thaw cycles, to eliminate any volatile residual gases. Exposure was done by filling the chamber through a leak valve to the desired pressure, with the uncorrected ion gauge signal transmitted to the computer, and converted to Langmuir units ($1\ \mathrm{L}=10^{-6}$ Torr s). The Kelvin probe was kept away from the surface during exposure that preceded $\Delta\Phi$-TPD measurement, due to calibration difficulties found otherwise. Blocking the Ru(001) surface by the vibrating Kelvin probe grid could result in a decrease of 45% in the molecular coverage relative to that of the bare surface, after identical exposure to methyl chloride.

III. RESULTS

A. Δp-TPD

Δp-TPD spectra following exposure of Ru(001) at 97 K to CH_3Cl are shown in Fig. 1 at a heating rate of 2.1 K/s. No dissociation products were detected in the gas phase, nor on the surface, after desorption, as revealed by $\Delta\Phi$ measurements (see below). At low coverage a single desorption peak (γ) appears, centered at 210 K. With increasing exposures this peak, which saturates around 1.6 L, shifts to lower temperatures (150 K), and marks the completion of the first monolayer (ML). At higher exposures a lower temperature desorption peak (β) is populated. This peak shifts from 150 K to 140 K as coverage increases and is saturated after 3 L exposure, suggesting similar population in this site as in the γ peak. Integrating the area under the Δp-TPD peaks, as the exposure increases, reveals that the sticking probability is coverage independent, and was assumed to be unity, as found for other methyl halide systems.[4–7] Further exposure

beyond the β peak saturation creates a third unsaturable peak (α), centered on 113 K, which is attributed to desorption of the condensed phase methyl chloride.

B. $\Delta\Phi$ measurements

Figure 2 summarizes the work function change data. In Fig. 2(A) $\Delta\Phi$ during adsorption of CH_3Cl on Ru(001) at 97 K is presented by a solid line. Up to 1.65 L a *decrease* of 1.88 V is observed, suggesting that in the first CH_3Cl layer the chlorine atoms point toward the surface. Subsequent methyl chloride exposure up to 3.2 L induces an *increase* of 0.4 V in the work function, attributed to the adsorption of second layer molecules. The majority of these molecules are thought to adsorb in a different orientation than those in the first layer, probably with the methyl pointing toward the surface. Maximum packing considerations reveal that the density of the first CH_3Cl layer (reached at an exposure of 1.6 L) is only 0.43 of its maximum value (see Sec. IV A below). This indicates that the second layer molecules have room to be in direct contact with the surface. However, the small $\Delta\Phi$ increase upon adsorption suggests that the equilibrium distance from the surface of the second layer molecules is somewhat larger compared with that of the first layer molecules. In addition, it is highly likely that these second layer molecules are less well ordered compared with the first layer adsorbates. As a result a nonnegligible fraction of these molecules may be at various orientations and tilt angles with respect to the surface normal. Further exposure in the range 3.2–5.5 L results in a *decrease* of the work function by 0.13 V following the adsorption of the third layer. This is a significant contribution, taking into account how far these molecules are from the surface.

A comparison between $\Delta\Phi_{ads}$ spectrum ($\Delta\Phi$ during adsorption of CH_3Cl) and the Δp-TPD spectra (Fig. 1) at the different initial exposures (coverages) reveals that the onset for the appearance of the β peak takes place slightly before the γ peak saturates. The minimum in the work function (1.65 L) lies in the middle of the narrow coverage range, where the two peaks populate simultaneously, and the β peak saturation is observed slightly before the local maximum in the $\Delta\Phi_{ads}$ curve (3.2 L). Additional exposure results in the population of the condensed phase multilayer α peak.

The work function change during $\Delta\Phi$-TPD of CH_3Cl from Ru(001) at a heating rate of 1.0 K/s is shown in Fig. 2(B). The $\Delta\Phi$ values measured at 97 K, after exposing the surface to the indicated doses in Langmuirs (L) (filled squares), closely follow the $\Delta\Phi_{ads}$ profile during continuous adsorption, as shown in Fig. 2(A). In order to identify the origin of work function change, whether caused by molecular rearrangement or due to molecular desorption, the onset temperatures for the CH_3Cl desorption as indicated by Δp-TPD are marked on the $\Delta\Phi$-TPD spectra by filled circles. No change in $\Delta\Phi$ at temperatures below the onset for the molecular desorption is observed at coverages, which correspond to doses lower than 1.4 L. This indicates that the methyl chloride molecules at that coverage regime ''wet'' the surface and have enough energy to overcome barriers for surface diffusion, resulting in homogeneously distributed molecules in the minimum energy configuration. The very

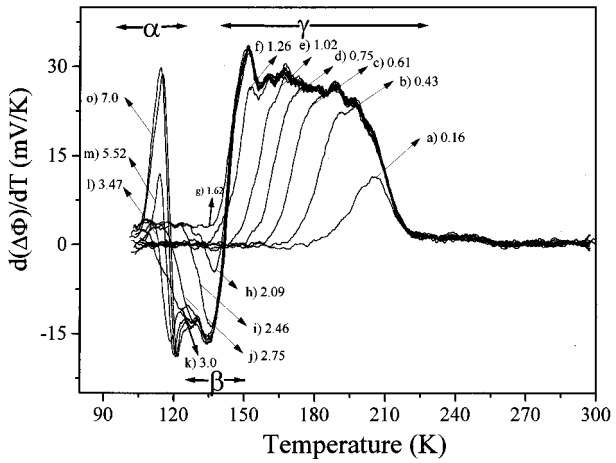

FIG. 3. Differential $\Delta\Phi$-TPD spectra $[d(\Delta\Phi)/dT]$ for the indicated exposures of CH_3Cl in Langmuirs. The adsorption temperature was 97 K and the heating rate 1.0 K/s.

good match (not shown) in the coverage dependence of the work function change between adsorption at 82 K ($\Delta\Phi_{ads}$) and desorption ($\Delta\Phi$-TPD) at that coverage regime has confirmed this observation. However, at higher exposures [1.68–3.47 L, Fig. 2(B) g–l], $\Delta\Phi$ increases linearly above 97 K, by as much as 0.11 V (for 1.68 L), with similar temperature dependence. This indicates that molecular rearrangement occurs *prior* to desorption.

In the inset of Fig. 2(B) the influence of the first two layers underlying the condensed phase layer on $\Delta\Phi$ is demonstrated by expanding the high coverage $\Delta\Phi$-TPD spectra between 105 K to 125 K. The local maximum in the $\Delta\Phi$-TPD spectra caused by the second layer desorption is shifted to higher temperatures with the increase in the condensed layer thickness.

Information obtained from $\Delta\Phi$-TPD experiments can be refined by differentiating the spectra versus temperature. As was demonstrated before,[15] it can be very closely correlated with the Δp-TPD spectra, especially in systems where interactions between adsorbates are weak. If the interactions are significant, as will be discussed below, the differences between the spectra may help us to understand the origin and the nature of these interactions. In Fig. 3 the $d(\Delta\Phi)/dT$ spectra are presented. The temperature range for each of the desorption peaks (α-γ) is also displayed. The main features of the Δp-TPD spectra are seen also in the $d(\Delta\Phi)/dT$ spectra, including the shift of the desorption peak to lower temperatures with increasing coverage. The negative and the alternating positive–negative contributions to $\Delta\Phi$, due to desorption from the β and α peaks, respectively, are clearly observed in the temperature range of 100–150 K.

IV. DISCUSSION

A. Adsorption of CH_3Cl on Ru(001)

In a previous study[4] we have found that a CH_3Br monolayer, adsorbed on Ru(001), contains $(3.6\pm0.3)\times10^{14}$ molecules/cm^2, equivalent to $CH_3Br/Ru=0.22\pm0.02$. Based on the similarity of the van der Waals radii of Br and Cl (1.95 Å and 1.86 Å,[16] respectively), and the similar dipole

moments of CH_3Br and CH_3Cl (1.82 D and 1.89 D, respectively),[17] which dominate the packing density through the dipole–dipole repulsion, we consider the CH_3Br coverage on Ru(001) a reasonable estimate for the monolayer coverage of CH_3Cl/Ru(001). This assumption is needed since the surface concentration of CH_3Cl could not be determined independently in our experiments. The maximum molecular density of CH_3Cl, arranged on a hexagonal close packed structure, is 8.34×10^{14} molecules/cm^2, based on molecular crystallographic data.[18] Therefore the density of the first CH_3Cl monolayer (saturated around 1.6 L) is only 0.43 from its maximal value.

Information on the dipole moment and polarizability of the methyl chloride upon adsorption at 97 K can be obtained by measuring $\Delta\Phi$ while exposing the sample to CH_3Cl. The work function *decreases* by 1.88 V upon completion of the first layer. It suggests that the CH_3Cl molecules adsorb with the chlorine atom pointing toward the surface.

Assuming free mobility of the adsorbates on the surface at 97 K, one expects a uniform, hexagonal arrangement of the adsorbates on the surface. This uniform distribution of parallel dipoles is a necessary condition to employ the electrostatic MC model,[11] and to evaluate the coverage dependence of the work function change. As in the Topping model,[12] the potential energy of an adsorbed dipole, which results from the electrostatic interaction with other dipoles in two-dimensional array of density n, can be calculated. Additionally, the stabilization energy due to the interaction with the image charge induced on the metal surface, which was neglected in the Topping model, is included in the model developed by Maschhoff and Cowin.[11]

The work function change, $\Delta\Phi$ is then given by the standard Helmholtz expression:

$$\Delta\Phi(n) = -4\pi\mu(n)n, \tag{1}$$

where

$$\mu(n) = \frac{\mu_0}{1+\alpha G(n)} \tag{2}$$

and

$$G(n) = F(n) - \frac{1}{4\beta^3 - \beta d^2} \tag{3}$$

and

$$F(n) = \frac{4\pi}{\sqrt{3}CR_s(n)^3}\left[1 + \frac{1}{\left[1+\left(\frac{2\beta}{CR_s(n)}\right)^2\right]^{3/2}}\right]. \tag{4}$$

$F(n)$ depends on the adsorbate surface geometry, and describes the characteristics of the electric field due to the other dipoles. For an hexagonal array of dipoles one obtains[11]

$$R_s(n) = (4/3)^{1/4}/\sqrt{n}, \qquad C = 0.658. \tag{5}$$

μ_0 is the dipole moment of the isolated adsorbate (approaching the zero-coverage limit), excluding its self-image dipole field effect. $\mu(n)$ is the dipole moment, which includes the image dipole effect, and that of neighbor adsorbates at density n. α is the molecular polarizability, assumed to be coverage independent (for a discussion on this issue see Ref. 19). β is the distance of the dipole center from its image plane and d is the molecular dipole length. It is important to note that the term $1/(4\beta^3-\beta d^2)$ in Eq. (3) is the major difference between the MC and the Topping models. This term arises from the stabilization due to interaction of the dipole with the screening (image) charge, induced on the metal surface. Consequently, the dipole moment at zero-coverage limit ($\mu(0)$), including the image dipole field effect, is *higher* than μ_0.

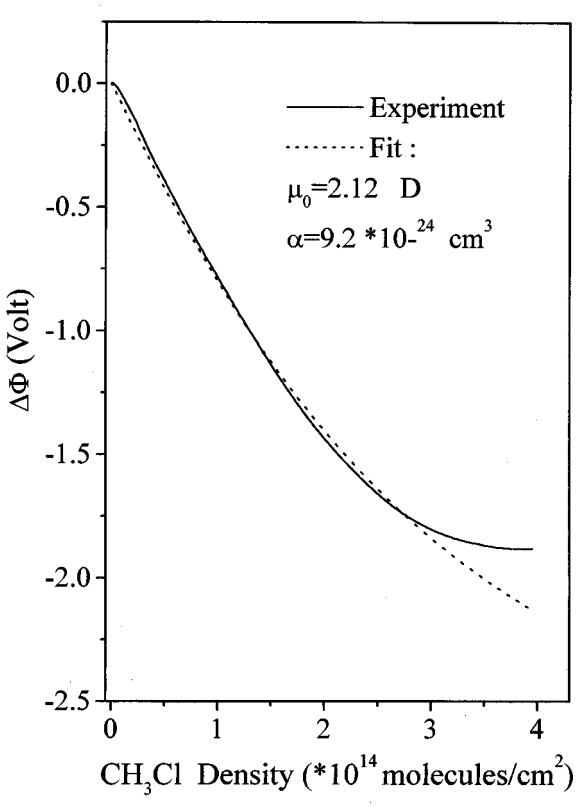

FIG. 4. A comparison of the change in $\Delta\Phi$ as a function of CH_3Cl density during its adsorption on Ru(001) at 97 K: measured (solid line) vs fitted, with least squares nonlinear procedure, according to Eqs. (1)–(5) (dotted line).

The C–Cl bond length in CH_3Cl is 1.77 Å.[16] Taking the van der Waals radius of the Cl atom to be 1.86 Å,[16] we set $\beta = 2.75$ Å and $d = 1.75$ Å as fixed parameters. As noted above, we assume $n = 3.6\times10^{14}$ molecules/cm^2 to be the 1 ML density of methyl chloride molecules on the Ru(001) surface.

In order to simulate the work function change data using the MC model, we are left with two free parameters: μ_0 and α. Figure 4 presents the comparison of the change in $\Delta\Phi$ as a function of CH_3Cl density during adsorption at 97 K: measured (solid line) versus the simulated curve, based on Eqs. (1)–(5) (dotted line). We have used a least squares nonlinear procedure in order to obtain the best fit. The parameters obtained are $\mu_0 = 2.12$ D (1 D $= 3.34\times10^{-28}$ C cm) and $\alpha = 9.2\times10^{-24}$ cm^3 (compared with gas phase values of 1.89

D and $4.72\times10^{-24}\,\mathrm{cm}^3$,[17] respectively). The sensitivity of the simulated $\mu(n)$ to the other parameters in the MC model was tested. The most important parameter has been the value of μ_0. Other paramters which were kept fixed (β and d, explained above) were found to have a smaller effect on $\mu(n)$. At coverages higher than 0.85 ML (3×10^{14} molecules/cm^2), the experimental points deviate from the simulated line, being at higher work function than that predicted by the MC model. Positive contribution to $\Delta\Phi$ due to the simultaneous population of the second layer could be responsible to this deviation. Both the dipole moment of the isolated molecule, and the polarizability, are higher than the corresponding gas-phase values. Larger dipole moment and polarizability of the adsorbed methyl chloride relative to its gas-phase values, reflect the electronic structure redistribution exerted at the adsorption site as a result of the molecule-metal bond formation.[11]

CH_3I was reported to be tilted with respect to the surface normal on Cu(111) based on HREELS measurements.[20] Furthermore, a change in adsorption geometry with coverage was found by RAIRS for CH_3I,[21,22] and CH_3Br,[23] on Pt(111). French *et al.*[22] reported that CH_3I is tilted by 42° with respect to the Pt(111) surface normal, at coverages less than 0.4 ML (1 ML was defined as $CH_3I/Pt=0.19$). This tilt angle gradually shifted to 18° at 1 ML. The decreasing tilt angle may be attributed to the growing repulsion as coverage increases (packing constraints), due to decreasing average distance between neighbor adsorbates. In our system we have no direct evidence for the orientation of the molecules on the surface. However, in order to explain the experimental work function change measurements, any tilt angle (ϕ) from the surface normal should be associated with a larger molecular dipole moment, by a factor of $1/\cos(\phi)$, compared with the perpendicular adsorption geometry. For a tilt angle of 45°, this would correspond to a dipole moment $\mu_0=3.0\,\mathrm{D}$, a significant deviation from the gas-phase value. If such coverage dependent tilt would have been the case in the current system of CH_3Cl on Ru(001), one would expect the *experimental* work function to become increasingly larger than the values predicted by the MC model as coverage increases, due to the increased dipole moment as the molecule shifts to a normal adsorption geometry. This prediction is in contrast to the observation demonstrated in Fig. 4.

A support for the validity of our claim that the molecular tilt can be inferred from work function change measurements was demonstrated also in the study of $CH_3Br/Cu(2ML)/Ru(001)$.[24] In this study a dipole moment estimate of $\mu(0)=1.55\,\mathrm{D}$ was extracted from the data. This dipole moment is smaller than the gas-phase value of 1.82 D.[17] This can be explained only on the basis of adsorption geometry arguments which favor some degree of tilt of the adsorbed molecule on the Cu(2 ML)/Ru(001) surface, in agreement with measurements performed on the $CH_3Br/Cu(111)$ system.[20]

We conclude that a vertical adsorption geometry of CH_3Cl on Ru(001) up to a coverage of 0.85 ML is consistent with our data and with its interpretation using the electrostatic MC model. This in spite of being at variance with the vibrational spectroscopy measurements performed on other methyl halides cited above.[20–23]

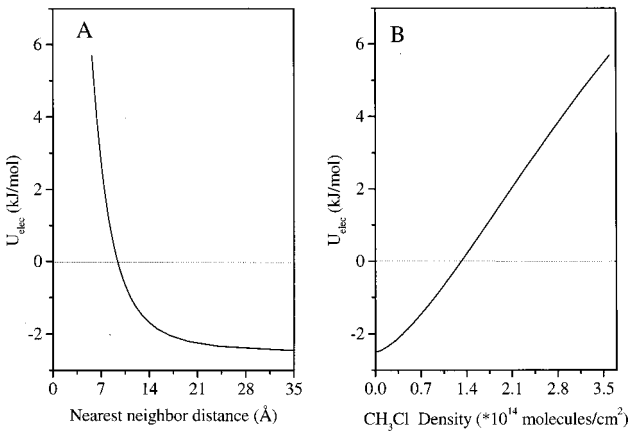

FIG. 5. (A) The calculated values of U_{elec} vs nearest neighbor separation distance. (B) Values calculated vs CH_3Cl density according to Eq. (7). The fitting parameters are $\mu_0=2.35\,\mathrm{D}$ and $\alpha=8.1\times10^{-24}\,\mathrm{cm}^3$.

B. Δp-TPD analysis

Interaction between adsorbed molecules is expected to lead to coverage dependence of the activation energy for desorption, $E_a(n)$. If we assume a coverage independent pre-exponential factor, ν, $E_a(n)$ can be extracted by inverting a Δp-TPD peak profile.[13] The first order desorption rate is expressed as follows:

$$-\frac{dn}{dt}=n\nu\exp\left(\frac{-E_a(n)}{RT}\right). \tag{6}$$

First, we normalize the spectrum to a well-defined coverage, preferably 1 ML saturation coverage. In our case, due to second layer population onset, prior to the completion of the first layer, the analysis has been limited to coverages up to 0.85 ML. Then we integrate the rate of desorption over time, dn/dt, to obtain $n(t)$. Finally, knowing $T(t)$ (at a particular heating rate), and the rate of desorption at every time step, enable us to extract $E_a(n)$ after inserting $\nu=2\times10^{13}\,\mathrm{s}^{-1}$. This number was obtained from Redhead[25] analysis, at close to zero-coverage limit.

The coverage dependence of the pre-exponential factor was studied for the $CH_3Br/Pt(111)$ system,[23] and was found to vary only weakly (30%) relative to the central value ($1\times10^{13}\,\mathrm{s}^{-1}$) at the 0.08–0.85 ML coverage range. This observation makes the assumption of constant pre-exponential factor reasonable. The average potential energy per dipole U_{elec}, in a homogeneous 2D array of adsorbates, with the dipole center placed at a distance β above the image plane of the metal, is given by:[11]

$$U_{\mathrm{elec}}(n)=\frac{\mu_0^2}{8\pi\epsilon_0}\left[\frac{1}{G(n)^{-1}+\alpha}\right]. \tag{7}$$

In Fig. 5 the average potential energy per dipole, U_{elec} is shown as a function of nearest neighbor distance [Fig. 5(A)] and of CH_3Cl molecular density [Fig. 5(B)]. The energy of the dipole is dictated by two contributions: the interaction energy with similar neighbor dipoles, assumed to align parallel to the surface normal, and by the field (affecting in the opposite direction to that of the dipole), which is induced by

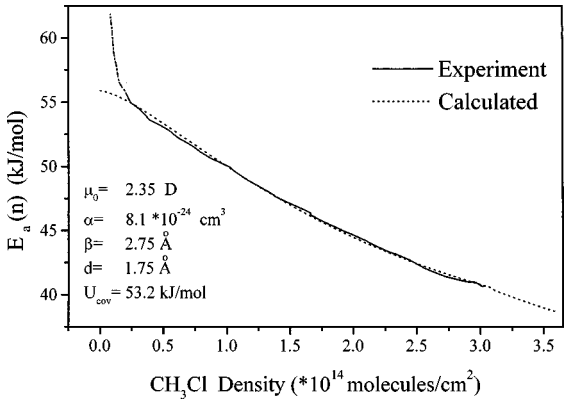

FIG. 6. Calculated [dotted line, according to Eq. (8)] and experimental E_a values (solid line, obtained from simulation of a Δp-TPD spectra at initial coverage of 0.85 ML) as a function of CH_3Cl density. The indicated parameters used for the calculation were extracted by employing a nonlinear least square fit between the calculated and experimental values. The fit excluded the lower coverage regime (dashed-dotted line) where sharp increase of the experimental values were obtained due to defects sites (see text).

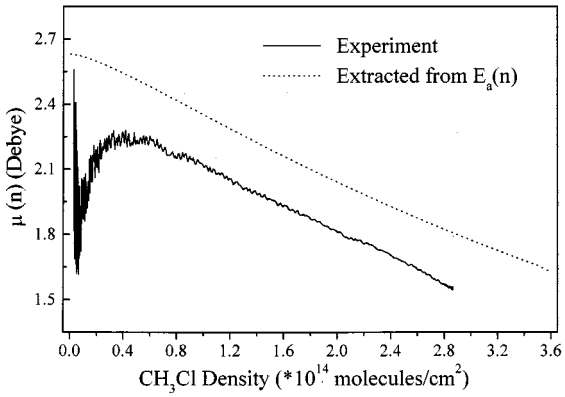

FIG. 7. The coverage dependent dipole moment of CH_3Cl, $\mu(n)$, extracted from a single a $\Delta\Phi$-TPD run, taken at heating rate of 1.0 K/s with initial coverage of 0.85 ML (solid line). The calculated $\mu(n)$ is based on $E_a(n)$ which have been derived from Fig. 6.

the images of all adsorbed dipoles, including the molecular dipole itself. The first contribution is repulsive while the second is attractive. These two opposite effects are included in U_{elec} [through $G(n)$, see Eq. (3)]. At the zero-coverage limit, U_{elec} is negative (-2.5 kJ/mol), meaning that the attraction between the dipole and its image dominates over the repulsion between adsorbates. With increasing coverage and decreasing nearest neighbor distance, the dipole–dipole repulsive interaction term becomes dominant and U_{elec} becomes positive up to 6 kJ/mol at coverages approaching 1 ML CH_3Cl/Ru(001). At infinite density $\mu(n)$ goes to zero while U_{elec} converges to $\mu_0^2/8\pi\epsilon_0\alpha$(20.2 kJ/mol), and the energy per molecule becomes the change in internal energy,[11] as a result of the complete depolarization of the initial dipole, reducing the dipole moment from μ_0 down to zero.

The binding energy of such a molecular dipole is expressed as a sum of an isolated molecule ''bonding'' (U_{cov}) and electrostatic (U_{elec}) energy terms $U_{\text{tot}}=U_{\text{elec}}+U_{\text{cov}}$. The variation of the activation energy for desorption with coverage arises from the change in the total energy of the system (nU_{tot}) upon removal of a single dipole.[26] Thus the activation energy is given by

$$E_a(n)\approx -\frac{d(nU_{\text{tot}}(n))}{dn}=-\frac{d(nU_{\text{elec}}(n))}{dn}-U_{\text{cov}}, \qquad (8)$$

where U_{cov} is fixed and corresponds to the binding energy of the isolated molecule in the absence of all interaction attributable to permanent dipole interactions. In Fig. 6 the activation energy for desorption as a function of surface density as derived from lineshape analysis of a single inverted Δp-TPD run at initial coverage of 0.85 ML is presented (solid line). In dotted line, the calculated curve of the activation energy for desorption, E_a, as a function of molecular density, based on Eq. (8) is shown. The fixed parameters used in the nonlinear least squares fit are: $\beta=2.75$ Å, $d=1.75$ Å. These parameters were chosen to be identical to those used for the analysis of $\Delta\Phi_{\text{ads}}$, shown in Fig. 4. The best agreement between the experimental data and the calculated values was achieved with $\mu_0=2.35$ D and $\alpha=8.1\times10^{-24}$ cm^3 (compared with gas phase values of 1.89 D and 4.72×10^{-24} cm^3, Ref. 17, respectively) and $U_{\text{cov}}=53.2$ kJ/mol. We note that these values are in good agreement with those extracted from the adsorption ($\Delta\Phi_{\text{ads}}$) experiment ($\mu_0=2.12$ D and $\alpha=9.7\times10^{-24}$ cm^3). The 11% and 20% deviations in the best fit values obtained for μ_0 and α, respectively, while employing a single electrostatic model to simulate two different measurables (desorption rates and work function change) are rather small and should be considered within the uncertainty level of the MC model.

The activation energy for desorption decreases from 55.9 kJ/mol at zero-coverage limit down to 38.6 kJ/mol at 1 ML. The sharp increase of the experimental values at the lowest coverages (<0.08 ML) is attributed to desorption from defect sites with higher binding energy.[9] This effect, which is observed in work function change measurements as well, will be discussed below, in Sec. IV C 1.

C. The correlation between Δp-TPD and $\Delta\Phi$-TPD spectra

1. Extraction of $\mu(n)$ from $E_a(n)$

Increased dipole–dipole repulsion was shown to lower the activation energy for desorption by 17.3 kJ/mol upon monolayer completion, due to destabilization of the molecule-surface bonding. Another possible effect of dipole–dipole repulsion is the tendency of similar dipoles to reduce charge separation (depolarization) in order to minimize the repulsion between adsorbates. The dependence of the activation energy for desorption on dipoles density (n), can be written in terms of $\mu(n)$. This is achieved by analytical calculation, based on Eqs. (7) and (8), after normalization by $1/8\pi\epsilon_0$:

$$Ea(n)\approx -\frac{d(nU_{\text{tot}}(n))}{dn}=\mathbf{a}\mu(n)^2+\mathbf{b}\mu(n)+\mathbf{c},$$
$$\mathbf{a}=-n\frac{dG(n)}{dn}\quad \mathbf{b}=-\mu_0 G(n),\quad \mathbf{c}=-U_{\text{cov}}. \qquad (9)$$

In Fig. 7 the experimental $\mu(n)$, as derived from a

single $\Delta\Phi$-TPD spectrum is shown as a solid line, based on relations given in Eqs. (1)–(5). The molecular density, n, is extracted by integrating a corresponding Δp-TPD spectrum at identical initial coverage of 0.85 ML. The dipole moment is shown to decrease from 2.44 D at zero coverage to 1.27 D (by extrapolation) at full monolayer. Around 0.12 ML [$CH_3Cl/Ru(001)=0.025$], a sharp decrease in the dipole moment is seen as coverage approaches zero. It looks as if the $\Delta\Phi$ per adsorbate strongly decreases at this coverage. It correlates with the sharp increase in the activation energy observed at lower coverages in Fig. 6, and contradicts the behavior one would expect based on the weaker dipolar interaction in that coverage regime. This sharp decrease is attributed to molecules attracted to defects. These can cause different adsorption geometry (e.g., large tilt angle), which results in both higher binding energy, as seen in Fig. 6, and in reduced dipoles.[27]

If the model is consistent with *both* $\Delta\Phi$-TPD and Δp-TPD experimental data, it is possible to extract the expected coverage dependence of the dipole moment, $\mu(n)$, from $E_a(n)$, solving the equation which relates $\mu(n)$ to $E_a(n)$ [Eq. (9)]. Indeed, this procedure is employed and the calculated $\mu(n)$ is shown as a dotted line in Fig. 7. We note that the slope of both curves, which is dictated by the coverage dependence of the dipolar interaction, is practically identical. This indicates that density dependence of both phenomena are described properly by the MC model, and that the $E_a(n)$ and $\mu(n)$ are correctly related, since they originate from the same electrostatic interactions. However, the fact that the calculated curve is shifted upwards indicates that the model overestimates μ_0 by 10%. This small discrepancy may arise from neglecting possible coverage effect in the pre-exponential factor of the desorption rate constant and in U_{cov}, as calculated by the MC model.

The nice fit of the MC model to two rather different experimental observables, using the same set of free parameters emphasizes the additional insight that can be gained by combining work function change with normal thermal desorption studies. However, in order to do so, a careful calibration has to be performed between the two measurable quantities over the entire coverage range.

Finally, we note that studies of systems where the electrostatic adsorbate–surface interaction is particularly strong, e.g., K/Re(001),[28] have shown that an attempt to simulate the work function change with coverage within the MC model has been only qualitatively successful. This can be rationalized by the questionable validity of the Topping model[12] and its extension[11] for systems where the nature of *local* interactions within the adsorbate-surface complex, its image and neighbors, can not be treated on the basis of simple dipole–dipole interactions.

2. $d(\Delta\Phi)/dT$ interpretation

The good correlation found between Δp-TPD and $\Delta\Phi$-TPD spectra provides the opportunity to examine simultaneously the desorbing CH_3Cl molecules (Δp), and those molecules which remain adsorbed on the surface ($\Delta\Phi$), during the course of a TPD experiment. In order to do so the derivative of $\Delta\Phi$ with respect to time is calculated using Eq. (1) after conversion to SI units:

$$\frac{d(\Delta\Phi)}{dt}=\frac{d(\Delta\Phi)}{dT}\cdot\frac{dT}{dt}$$
$$=-\frac{1}{\epsilon_0}\cdot\frac{dT}{dt}\left(\mu(n)\frac{dn}{dT}+n\frac{d\mu(n)}{dT}\right). \qquad (10)$$
$$\text{(i)} \qquad \text{(ii)}$$

The above equation consists of two separate contributions to $\Delta\Phi$:

(i) A product of the rate of desorption ($-dn/dT$), which is identical to the Δp-TPD signal, and the CH_3Cl dipole moment at a specific surface density. This term reflects the change in $\Delta\Phi$ due to the decreasing surface coverage (molecules that leave the surface) during thermal desorption. (ii) A product of the surface density and the derivative of the coverage-dependent dipole moment with respect to time. This term reflects the change in $\Delta\Phi$ which arises from the rearrangement of the adsorbed molecules, which are left on the surface while the coverage decreases during desorption, induced by modifications in their local environment (e.g., smaller dipole–dipole interaction, changing tilt angle, etc.).

The use of work function change derivative was previously employed to study the desorption kinetics of CO/Ru (001),[15] where the dipole moment has only minor coverage dependence due to the weak dipole–dipole interactions. The dipole moment of CO on the Ru(001) surface is considerably lower then that of the methyl halides and can be estimated, according to Eq. (1), to be $\mu=-0.22$ D. In such a case [up to $CO/Ru(001)=0.33$] Eq. (10) reduces to a simple linear relation between the rate of change of $\Delta\Phi$ with time and the rate of desorption, producing a good overlap between the two types of spectra.[15]

Knowing the temperature (time) dependence of the surface density, $n(t)$, during the course of Δp-TPD, we can express $\mu(n)$, found by the MC model (see Fig. 7), in terms of $\mu(t)$, and represent separately the two time (temperature)-dependent terms of Eq. (10). In Fig. 8(A), the simulated $\Delta\Phi$-TPD, [Fig. 8(A a)] and Δp-TPD [Fig. 8(A d)] spectra are shown for initial CH_3Cl coverage of 0.85 ML. In addition, the first (i) and the second (ii) terms of Eq. (10) [Figs. 8(A b) and 8(A c), respectively] are presented as well. For clarity of presentation the second term is multiplied by (-1). Additionally, the values for $\mu(n)$ are multiplied by 0.9, in order to compensate for the 10% overestimate in the calculation of $\mu(0)$, as shown in Fig. 7 (see discussion above). We note that the measured quantities [$-dn/dT$ and $d(\Delta\Phi)/dT$] are related to the rate of desorption ($-dn/dt$) and the rate of work function change ($d(\Delta\Phi)/dt$) through the heating rate (dT/dt), which was kept fixed at 1.0 K/s in both experiments.

During the thermal desorption process depolarization effects are reduced upon decreasing the surface molecular density, n. As a result, two phenomena, represented by the two terms of Eq. (10), are noticed with opposite contribution to $\Delta\Phi(n)$: increase of the dipole moment [$\mu(n)=-\Delta\Phi(n)/$

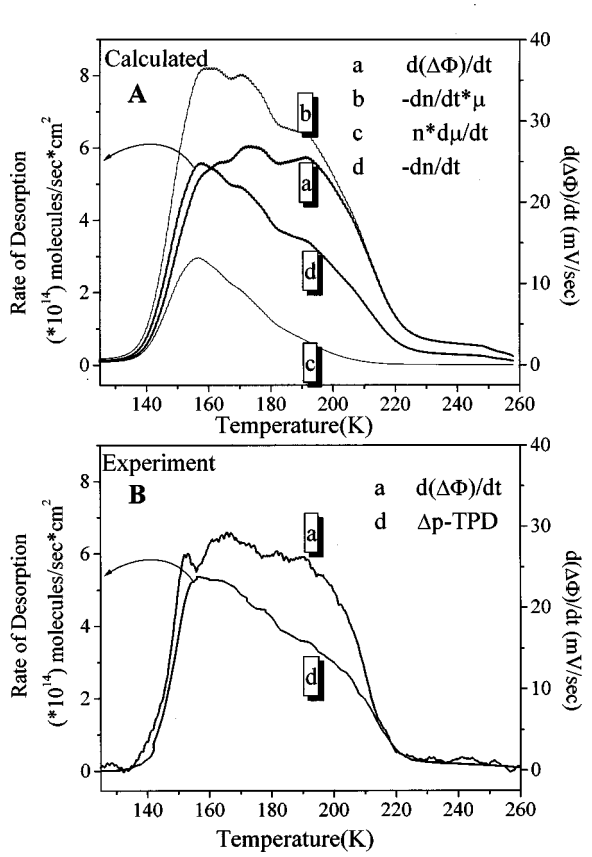

FIG. 8. (A) A comparison of $[d(\Delta\Phi)/dt]$, simulated on the basis of $\mu(n)$, seen in Fig. 7, with Δp-TPD. The two terms of Eq. (10), (i) and (ii), are shown as a function of temperature as well. (B) Corresponding experimental $d(\Delta\Phi)/dt$ and Δp-TPD spectra. Both experimental spectra were obtained at an initial CH_3Cl coverage of 0.85 ML, adsorption temperature of 97 K, and a heating rate 1.0 K/s.

$\epsilon_0 n$] of the adsorbed CH_3Cl molecule with diminishing density leads to an *increase* in $\Delta\Phi$, as contributed by each of the desorbing molecules. Concomitantly, it leads to a $\Delta\Phi$ *decrease* per single CH_3Cl molecule that remained adsorbed on the Ru(001) surface, which becomes less depolarized by its neighboring adsorbates. Note that $d(\Delta\Phi)/dt$ and the first and second terms in Eq. (10) are presented in Fig. 8(A) by *a*, *b*, and $-c$, respectively.

In order to examine the adequacy and rationale behind the demonstration in Fig. 8(A) one has to compare the profiles of the corresponding simulated Δp-TPD$(-dn/dT)$ and $d(\Delta\Phi)/dT$ spectra [Fig. 8(A d) and 8(A a), respectively] with the experimental data. In Fig. 8(B) the two experimentally obtained spectra of $d(\Delta\Phi)/dt$ [Fig. 8(B a)] and Δp-TPD [Fig. 8(B d)] are shown to have very good correlation with the simulated spectra shown in Fig. 8(A a) and 8(A d). This analysis further substantiates the main theme of this work, namely the ability to correlate the coverage dependence of the dipole moment and of the activation energy for desorption under the framework of a single electrostatic (MC) model.

Finally, we note that the difference between $d(\Delta\Phi)/dt$ and Δp-TPD signals becomes more significant above 155 K with decreased surface molecular density (increasing temperature). The first term in Eq. (10) (i) is a product of the dipole moment and the rate of desorption. They change in an opposite direction when CH_3Cl density decreases. The difference between them is attributed to the strong density dependence of the dipole moment and to the decreasing contribution of the second term (ii) to $\Delta\Phi$ with decreasing molecular density.

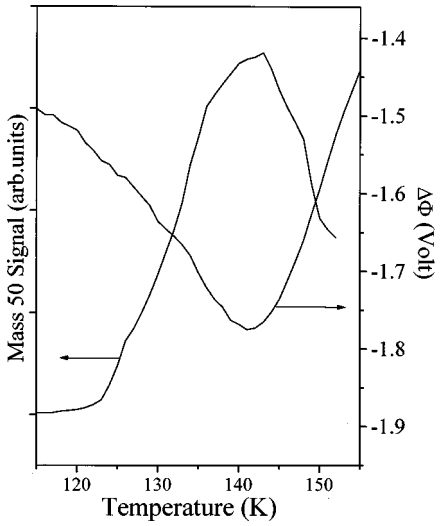

FIG. 9. A comparison of Δp-TPD and $\Delta\Phi$-TPD at the second layer desorption temperature regime (115 K–155 K) after 3.0 L exposure of CH_3Cl on Ru(001) at 97 K.

3. Molecular rearrangement

Rearrangement of adsorbed molecules during sample heating is expected if the molecules are bound to the surface in an energetically metastable structure upon adsorption at low crystal temperatures. Comparison of the directly measured $\Delta\Phi_{ads}$ during the adsorption of CH_3Cl on Ru(001) at 97 K [see Fig. 2(A)], to the work function change, extracted from the $\Delta\Phi$-TPD curve, reveals that up to 0.85 ML the $\Delta\Phi$ values are identical. This is not surprising if we assume that the molecules have close to unity sticking probability. Wetting the surface, while reducing the surface free energy, is thus the major energetic driving force for adsorption. This leads to a formation of uniformly distributed array of 2D dipoles (provided that barriers for diffusion do not prevent free migration of the adsorbates at 97 K). However, beyond 0.85 ML there is a significant difference between the two. In Fig. 9 the Δp-TPD and $\Delta\Phi$-TPD spectra obtained following exposure of 3.0 L CH_3Cl/Ru(001) are shown in the temperature range of 115–155 K. In this temperature range most of the second layer molecules (β peak) desorb. This should lead to $\Delta\Phi$ decrease upon surface heating, a mirror behavior to the work function increase observed during adsorption.

A *minimum* in $\Delta\Phi$ is observed exactly at the temperature where the β peak desorption rate is at its maximum (143 K). If this desorption would have precisely followed the work function change profile during second layer adsorption, a *maximum rate* of $\Delta\Phi$ decrease would have been expected in the same temperature (143 K). The $\Delta\Phi$ minimum under these conditions should appear at higher temperature around 152 K.

The lack of consistency between the two spectra is revealed by the shift of the $\Delta\Phi$-TPD minimum toward lower temperatures. This shift may be explained by rearrangements within the *multilayer* CH_3Cl molecules, which result in their migration perpendicular to the surface to occupy second layer sites which have been partially depopulated during the second layer desorption. This process leads to an early (lower temperature) increase in the work function, which outweighs the $\Delta\Phi$ decrease caused by second layer desorption.

If we limit the adsorption to exposure sufficient to reach the minimum in the $\Delta\Phi$ adsorption curve (1.65 L) and run $\Delta\Phi$-TPD, we obtain the spectrum seen in Fig. 2(B g). It is evident that a linear increase in $\Delta\Phi$ is observed *prior* to molecular desorption, which can be attributed to rearrangement within the *first* layer molecules. The last 0.3 L adsorbed on the surface prior to first layer completion induces this rearrangement, which still takes place concurrently with the first stage of second layer build up.

Upon adsorption at 97 K the molecules are thought to be distributed in a homogeneous 2D arrangement on the surface. This, we believe, is the case up to a coverage of 0.85 ML. At higher coverages an unstable layer is formed. Since the increase of the work function is linear with temperature [see Fig. 2(B g) at $T<143$ K], a pure thermally activated flipping mechanism, as suggested for the ''Br down'' to ''methyl down'' of CH_3Br molecules on Ru(001)[4] is not feasible. Annealing the surface supplies energy to overcome the barrier for diffusion leading to a more stable configuration. The increase in $\Delta\Phi$ may also be due to transfer of population away from the first layer, governed by reducing dipole–dipole repulsion.

V. CONCLUSIONS

Work function change measurements ($\Delta\Phi$) combined with temperature programmed desorption (TPD) were employed to study the layer growth mechanism and the CH_3Cl dipole–dipole interactions on Ru(001) over the temperature range of 97 K–230 K. The activation energy for desorption (E_a) and the molecular dipole moment (μ) decrease from 55.9 kJ/mol and 2.44 D at the zero-coverage limit to 38.6 kJ/mol and 1.27 D at one monolayer coverage. This coverage dependence originates from strong dipolar lateral repulsion among neighbor CH_3Cl molecules. Using an electrostatic model, developed by Maschoff and Cowin (MC model), the dipole moment of the isolated molecule (excluding image dipole effect), μ_0 (2.35 D), and the polarizability, $\alpha(8.1\times10^{-24}\,\mathrm{cm}^3)$, of methyl chloride were extracted from TPD data. These numbers may be compared with μ_0 (2.12 D), and the polarizability, $\alpha(9.2\times10^{-24}\,\mathrm{cm}^3)$ extracted from work function data, based on the same model. The full coverage dependence of the dipole moment, $\mu(n)$, simulated based on μ_0 and α, agreed very well with the coverage dependent dipole moment extracted from work function change measurements over the coverage range of 0.1–0.85 ML. The temperature derivative spectra of the $\Delta\Phi$-TPD curves $[d(\Delta\Phi)/dT]$ are presented and shown to follow the shift of the sub-monolayer Δp-TPD peak to lower temperatures. Measuring the dependence of the dipole moment on coverage and temperature, one can correlate the two TPD spectra and learn about the factors that govern these dependencies.

A vertical adsorption geometry of CH_3Cl on Ru(001) over a wide coverage range is concluded to be consistent with both Δp-TPD and $\Delta\Phi$-TPD measurements as analyzed by the MC model.

ACKNOWLEDGMENTS

This research has been partially supported by a grant from the German–Israeli Foundation and the Israel Science Foundation. The Farkas Center for Light Induced Processes is supported by the Bundesministerium für Forschung und Technologie and the Minerva Gesellschaft für die Forschung mbH.

[1] B. E. Bent, Chem. Rev. **96**, 1361 (1996).
[2] F. Zaera, Acc. Chem. Res. **25**, 260 (1992).
[3] Y. Zhou, M. A. Henderson, W. M. Feng, and J. M. White, Surf. Sci. **224**, 386 (1989).
[4] T. Livneh and M. Asscher, J. Phys. Chem. B **101**, 7505 (1997).
[5] M. A. Henderson, G. E. Mitchell, and J. M. White, Surf. Sci. Lett. **184**, L325 (1987).
[6] A. Berko, W. Erley, and D. Sander, J. Chem. Phys. **93**, 8300 (1990).
[7] F. Solymosi, A. Berko, and K. Revesz, Surf. Sci. **240**, 50 (1990).
[8] E. V. Albano, J. Chem. Phys. **85**, 1044 (1985).
[9] P.-H. Lu, P. J. Lasky, Q.-Y. Yang, Y. Wang, and R. M. Osgood, Jr., J. Chem. Phys. **101**, 10145 (1994).
[10] W. Bruch, Surf. Sci. **125**, 194 (1983).
[11] B. L. Maschhoff and J. Cowin, J. Chem. Phys. **101**, 8138 (1994).
[12] J. Topping, Proc. R. Soc. London, Ser. A **114**, 67 (1927).
[13] B. L. Maschhoff, M. J. Ledema, and J. Cowin, Surf. Sci. **359**, 253 (1996).
[14] K. A. Magrini, S. C. Gebhard, B. E. Koel, and J. L. Falconer, Surf. Sci. **248**, 93 (1991).
[15] H. Pfnür, P. Feulner, and D. Menzel, J. Chem. Phys. **79**, 4613 (1983).
[16] L. Pauling, in *Nature of the Chemical Bond*, 3rd ed. (Cornell University Press, Ithaca, 1960), pp. 260.
[17] *Handbook of Chemistry and Physics*, 73rd ed., edited by D. R. Lide (CRC Press, Boca Raton, FL, 1993).
[18] T. Kawaguchi, M. Hijikigawa, Y. Hayafuji, M. Ikeda, R. Fukushima, and Y. Tomiie, Bull. Chem. Soc. Jpn. **46**, 53 (1973).
[19] R. W. Verhoef and M. Asscher, Surf. Sci. **391**, 11 (1997).
[20] J.-L. Lin and B. Bent, J. Vac. Sci. Technol. A **10**, 2202 (1992).
[21] F. Zaera, H. Hoffman, and P. R. Griffiths, J. Electron Spectrosc. Relat. Phenom. **54/55**, 705 (1990).
[22] C. French and I. Harrison, Surf. Sci. **342**, 85 (1995).
[23] C. French and I. Harrison, Surf. Sci. **387**, 11 (1997).
[24] T. Livneh and M. Asscher, J. Phys. Chem. B **103**, 5665 (1999).
[25] P. A. Redhead, Vacuum **12**, 203 (1962).
[26] H. J. Kreuzer, Langmuir **8**, 774 (1992).
[27] (a) R. Smoluchowsky, Phys. Rev. **60**, 661 (1941); (b) ''Work function of metals,'' J. Holzl and F. K. Schulte, in *Tracts in Modern Physics*, Vol. 85 (Springer, Berlin, 1979).
[28] R. W. Verhoef, W. Zhao, and M. Asscher, J. Chem. Phys. **106**, 9353 (1997).